Parity-Time Symmetry in a Single-Loop Photonic System

Zhiqiang Fan, Zheng Dai, Qi Qiu, and Jianping Yao, *Fellow, IEEE, Fellow, OSA*

***Abstract*—Non-Hermitian photonics based on parity-time (PT) symmetry has been considered an effective solution to achieve mode selection for optical or microwave single-mode oscillation. A PT-symmetric system is usually implemented using two mutually coupled elements with identical geometry or a single element based on precise longitudinal refractive index modulation. In this study, we propose a novel scheme to achieve PT symmetry based on polarization mode manipulation in a single optical loop. By controlling the polarization states of two light waves that are propagating along the clockwise (CW) and counter-clockwise (CCW) directions in the single optical loop, two equivalent mutually-coupled loops with identical geometry and a balanced gain and loss are formed. Based on this concept, a wavelength-tunable single-mode fiber laser with a sub-kHz linewidth is realized. The tunability is achieved by thermally tuning the wavelength of an integrated microdisk resonator (MDR) incorporated in the optical loop. Experimental results show that a continuously tunable single-mode laser with a sub-kHz linewidth of 640 Hz and a wavelength tuning range from 1552.953 to 1554.147 nm is realized. The key advantages of using a single optical loop to implement PT symmetry include greatly simplified implementation and highly improved stability. The demonstration opens new avenues to implement high-performance PT-symmetric systems for applications in photonic and microwave photonic systems.**

***Index Terms*—Fiber lasers, microwave photonics, parity-time symmetry, ring lasers.**

I. Introduction

NON-HERMITIAN Hamiltonians having parity-time (PT) symmetry open up the possibility of exploring fascinating phenomenon of non-Hermitian physics, due to its ability to describe complex quantum theories having positive probabilities and unitary time evolution [1], [2]. Thanks to the flexibility in controlling optical gain and loss, photonic and microwave photonic systems are ideal platforms for experimentally exploring novel functions of non-Hermitian systems based on PT symmetry [3]. Such explorations, in turn, enhance the comprehension of non-Hermitian physics, which helps advance the breakthroughs for photonic and microwave photonic applications. Single-mode optical [4]–[12] or microwave [13]–[15] oscillation is one critical application of PT symmetry to demonstrate its excellent mode selection ability.

In general, a PT-symmetric system can be implemented with a topology having transverse or longitudinal PT-symmetry [5]. In a transverse PT-symmetric system [6], there are two mutually coupled elements such as two microcavities or waveguides having an identical geometry. Its implementation is challenging since the two elements must have exactly identical geometry. In a longitudinal PT-symmetric system [7], the PT symmetry can be implemented in a single element such as a waveguide or a microcavity, in which the element is index modulated longitudinally. Its implementation is also difficult due to the requirement for precise refractive index modulation in the element.

A laser with a narrow linewidth is a crucial device for applications such as in optical communications [16], optical imaging [17], frequency synthesis [18], and optical spectroscopy [19]. The key challenge in implementing a laser with an ultra-narrow linewidth is to have an ultra-narrow optical filter in the laser cavity, which is extremely difficult to achieve. Recently, the concept of PT symmetry has been introduced to the field of photonics and has been employed to perform mode selection to achieve single-mode lasing [4]–[12]. Compared with the conventional implementations [20]–[24], PT-symmetry exhibits an outstanding advantage in terms of simplicity and flexible mode controllability. Up to now, all reported single-mode lasers based on PT symmetry are all implemented based on integrated photonics [4]–[11]. Since the cavity is very short, the linewidth is wide, making the lasers not be suitable for high-performance applications [16]–[19].

According to the Schawlow-Townes formula [25], a longer lasing cavity means a longer photon lifetime and a narrower laser linewidth. Therefore, an optical fiber laser with a long loop is a great choice to guarantee a narrow linewidth. However, a long loop will cause multiple closely spaced longitudinal modes. By employing transverse PT symmetry in an optical fiber laser, we may achieve single-mode lasing with a sub-kHz linewidth [12], but the implementation is challenging due to the fact that two loops with exactly an identical geometry are needed, making the

Manuscript received January 13, 2020; revised March 4, 2020; accepted March 20, 2020. Date of publication March 27, 2020; date of current version July 23, 2020. This work was supported by the Natural Sciences and Engineering Research Council of Canada (NSERC). The work of Z. Fan was supported by a scholarship from the China Scholarship Council. *(Corresponding author: Jianping Yao.)*

Zhiqiang Fan is with the Microwave Photonics Research Laboratory, School of Electrical Engineering and Computer Science, University of Ottawa, Ottawa, ON K1N 6N5, Canada, and also with the School of Optoelectronic Science and Engineering, University of Electronic Science and Technology of China, Chengdu 610054, China (e-mail: zfan033@uottawa.ca).

Zheng Dai and Jianping Yao are with the Microwave Photonics Research Laboratory, School of Electrical Engineering and Computer Science, University of Ottawa, Ottawa, ON K1N 6N5, Canada (e-mail: zdai049@uottawa.ca; jpyao@eecs.uottawa.ca).

Qi Qiu is with the School of Optoelectronic Science and Engineering, University of Electronic Science and Technology of China, Chengdu 610054, China (e-mail: qqiu@uestc.edu.cn).

Color versions of one or more of the figures in this article are available online at http://ieeexplore.ieee.org.

Digital Object Identifier 10.1109/JLT.2020.2982911

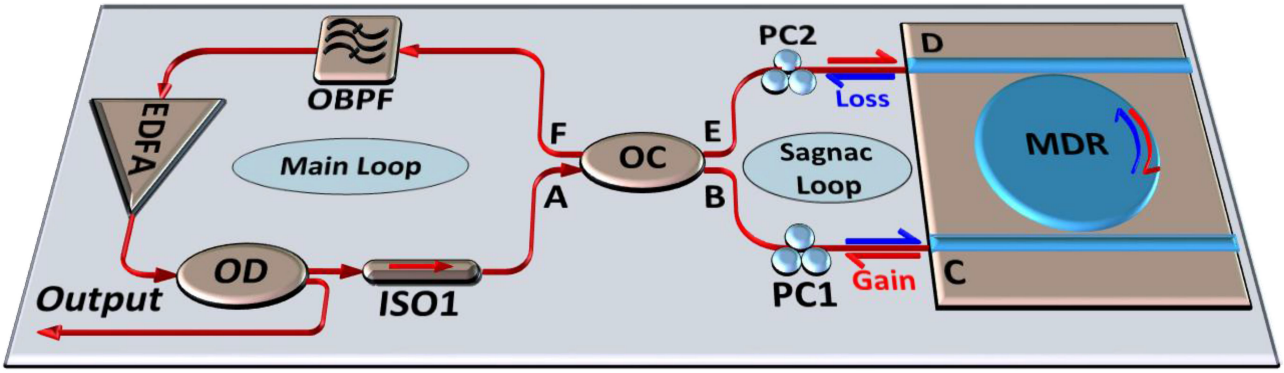

Fig. 1. Schematic diagram of the proposed single-loop PT-symmetric optical fiber laser. ISO: isolator; OD: optical divider; OC: optical coupler; PC: polarization controller; MDR: microdisk resonator; OBPF: optical bandpass filter; EDFA: erbium-doped fiber amplifier.

implementation difficult considering the long loop lengths of a fiber laser [6], [8]–[11].

Recently, we reported a new scheme to achieve a wavelength-tunable PT-symmetric fiber laser with a single optical loop based on an integrated microdisk resonator (MDR) [26], in which the single optical loop is a Sagnac loop and the tunability is realized by thermally tuning the MDR. The work reported in this article is an extension of the work in [26]. To be specific, in this paper an in-depth study of the wavelength-tunable PT-symmetric fiber laser, including the theoretical analysis and the performance demonstration, is performed.

The key to achieve PT symmetry in the fiber laser is to realize polarization mode manipulation in the Sagnac loop. By controlling the polarization states of two light waves propagating along the clockwise (CW) and counter-clockwise (CCW) directions in the Sagnac loop, two equivalent mutually-coupled loops with identical geometry are established. By controlling the gain and loss of the two equivalent loops to make them identical in magnitude, PT symmetry is realized. By making the gain or loss greater than the coupling coefficient, the PT-symmetry condition is broken, and one mode will be selected, and single-mode lasing is achieved. In the optical loop, an MDR implemented based on silicon on insulator (SOI) is incorporated, which is used to tune the lasing wavelength. The proposed fiber laser is experimentally demonstrated. Experimental results show that a continuously tunable single-mode laser with a sub-kHz linewidth of 640 Hz and a wavelength tuning range from 1552.953 to 1554.147 nm is realized.

II. Principle

Figure 1 shows the schematic diagram of the proposed single-loop PT-symmetric optical fiber laser. The fiber laser consists of a main loop and a Sagnac loop connected via an 3-dB optical coupler (OC). To achieve PT symmetry, two mutually coupled loops with one having a gain and the other having a loss are needed, which are implemented in the fiber laser using a Sagnac loop. As can be seen in Fig. 1, an erbium-doped fiber amplifier (EDFA) is used in the fiber laser as the gain medium. The amplified light wave from the EDFA is sent through an optical divider (OD), an isolator (ISO1), and an OC, to the Sagnac loop. Along the CCW direction, the light at port B of the OC is sent to an integrated MDR via a polarization controller (PC1), and transmitted to the drop port D of the MDR. The light from port D is transmitted through a second polarization controller (PC2) and the OC, and fed back to the EDFA via an optical bandpass filter (OBPF). Along the CW direction, the light at port E of the OC is sent to the MDR via PC2, and transmitted to the port C of the MDR. The light from port C is transmitted through PC1 and the OC, and fed back to the EDFA via the OBPF. Then, two loops, the CCW loop with the light path of A->B->C->D->E->F->A and the CW loop with the light path of A->E->D->C->B->F->A, are achieved in a single physical loop. Since only the transverse electronic (TE) mode can be supported in the bus waveguide of the MDR, by controlling the polarization states of the light waves entering the Sagnac loop from the CW and CCW directions by tuning the two PCs, the gain and loss coeffcients of two loops corresponding to the CW and CCW directions can be controlled to be identical in magnitude. Since the MDR supports only TE mode, the generated light is linearly polarized, and its polarization state would be fixed once the tuning of the PCs is stopped. The MDR is implemented on SOI and can be tunable by thermally tuning. The isolator is included in the main loop to ensure unidirectional operation. The OBPF is included in the main loop to define the wavelength tuning range and to filter out the amplified spontaneous emission (ASE) noise from the EDFA. The OD is used to tap part of the lasing light for performance evaluation. The optical spectrum is analyzed using an optical spectrum analyzer (OSA). The lasing mode and the linewidth of the output are analyzed based on the delayed self-heterodyne method.

In the time domain, the coupling mode equations of the *n*th-modes in the single-loop PT-symmetric laser are given by [6],

$$\frac{d}{dt}\begin{bmatrix} a_n \\ b_n \end{bmatrix} = \begin{bmatrix} -i\omega_n + g_{a_n}, & i\kappa_n \\ i\kappa_n, & -i\omega_n + g_{b_n} \end{bmatrix} \begin{bmatrix} a_n \\ b_n \end{bmatrix} \quad (1)$$

where a_n and b_n are the electrical fields of the *n*th-modes in the two equivalent mutually-coupled loops, ω_n is the eigen-frequency of the *n*th-modes, g_{bn} and g_{an} are the net gain and loss coefficients of the gain and loss loops, respectively, and κ_n is the coupling coefficient between the two loops for the *n*th-modes. Here we assume the CCW and CW loops are the loss

and gain loops, respectively. Then we have $g_{an} \propto \cos\alpha$ and $g_{bn} \propto \cos\beta$, where α is the polarization angle between the principal axis of the bus waveguide and the polarization direction of the light wave entering the MDR from port C, β is the polarization angle between the principal axis of the bus waveguide and the polarization direction of the light wave entering the MDR from port D. The coupling coefficient κ_n is a constant and determined by the 3-dB OC. By solving the coupling mode equations, the *n*th-eigenfrequencies of the PT-symmetric laser are given by

$$\omega_n^{(1,2)} = \omega_n + i\frac{g_{a_n} + g_{b_n}}{2} \pm \sqrt{\kappa_n^2 - \left(\frac{g_{a_n} - g_{b_n}}{2}\right)^2} \quad (2)$$

The PT-symmetry condition is achieved by tuning the gain of the gain loop to be equal to the loss of the loss one, that is. $g_{an} = -g_{bn} = g_n$, and thus Eq. (2) is rewritten as

$$\omega_n^{(1,2)} = \omega_n \pm \sqrt{\kappa_n^2 - g_n^2} \quad (3)$$

According to Eq. (3), the relationship between the *n*th-eigenfrequencies and the ratio between the gain or loss and the coupling coefficient is plotted in Fig. 2(a). An exceptional point (EP) is found when the gain or loss coefficient of the two loops is equal to the coupling coefficient, that is $g_n = \kappa_n$. If the gain or loss coefficient is lower than the coupling coefficient $(g_n < \kappa_n)$, any pair of lasing modes will undergo bounded neutral oscillation. That means that the PT symmetry is unbroken. In contrast, once the gain or loss exceeds the coupling coefficient $(g_n > \kappa_n)$, a conjugate pair of lasing and decaying modes are achieved. The PT-symmetry condition is broken. We assume that only the *0*th-modes, which have the largest gain, are under the condition of broken PT symmetry $(g_0 > \kappa_0)$, and the other modes are under the unbroken PT-symmetry condition $(g_n < \kappa_n, n \neq 0)$. Then, only *0*th-mode is selected to oscillate, and all the other modes are suppressed.

It should be noted, however, single-mode lasing can also be implemented in the absence of PT symmetry if the gain of one mode (primary mode) is greater than the loss, and the gains of the other modes are less than the losses. However, the gain contrast between the primary mode and the next competing mode is very small without PT symmetry. The small gain contrast puts forward a strict requirement on the 3-dB bandwidth of a bandpass filter for mode selection to ensure stable single-mode lasing. Assume that the gain contrast without PT symmetry is defined as $\gamma_s = g_0 - g_1$, where g_0 and g_1 are the gain coefficients of the primary mode and the next competing mode, respectively.

In contrast, the gain contrast (γ_{PT}) between the primary mode and the next competing mode would be significantly enhanced if the laser is in the condition of PT symmetry. The enhancement factor (G) for the gain contrast (γ_{PT}) is given by

$$\gamma_{PT} = \sqrt{g_0^2 - g_1^2} = G \cdot \gamma_s \quad (4)$$

$$G = \frac{\gamma_{PT}}{\gamma_s} = \sqrt{\frac{g_0/g_1 + 1}{g_0/g_1 - 1}} \quad (5)$$

where γ_{PT} and γ_S are the gain contrasts with and without PT symmetry, respectively. A simulation is performed to show the

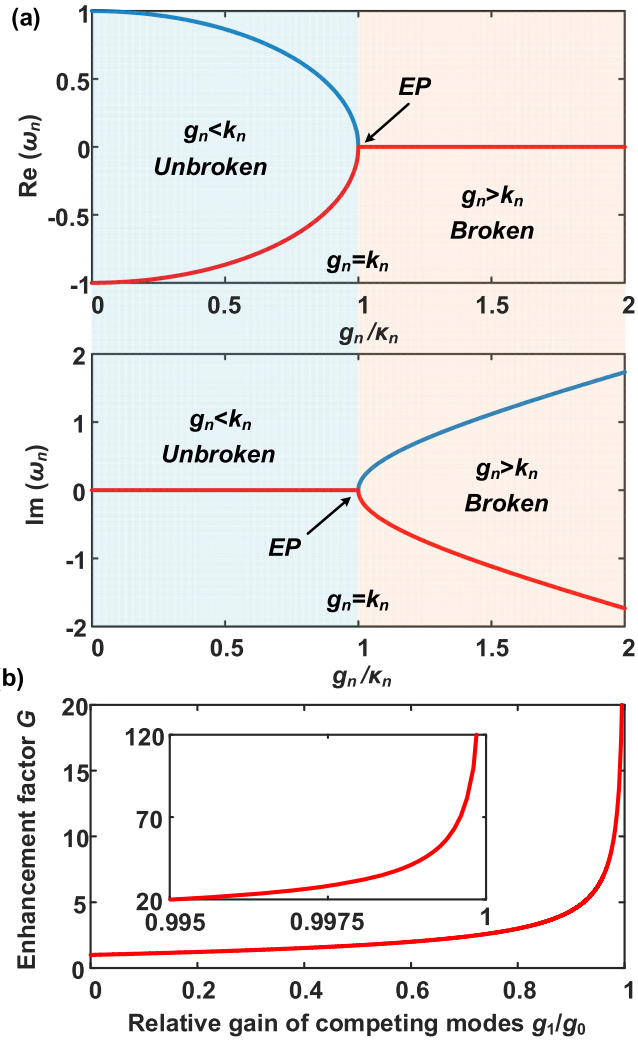

Fig. 2. (a) Real and imaginary parts of the *n*th-eigenfrequencies at the conditions of broken and unbroken PT symmetry. (b) Gain contrast enhancement with PT symmetry. EP: exceptional point.

enhancement factor *G* as a function of the relative gain between the primary mode and the next competing mode (g_1/g_0), as shown in Fig. 2(b). The value of g_1/g_0 is between 0 and 1. Thus, a value bigger than one is found for the enhancement factor *G*. In particular, a sharply increasing in the enhancement factor *G* is found when the gain of the next competing mode g_1 is close to the gain of the primary mode g_0. In other words, the gain contrast in the PT-symmetric laser is greatly enhanced, which provides an effective solution for mode selection, thus achieving a very stable single-mode lasing.

III. Experimental Results and Discussions

A proof-of-concept experiment is carried out based on the setup shown in Fig. 1. In the proposed single-loop PT-symmetric laser, the devices used in the demonstration are commercial off-the-shelf photonic components except for the MDR, which is custom designed. The EDFA (FiberPrime Inc. EDFA-C-14-S-FA) has a 25-dB gain and a 13-dBm saturated output power.

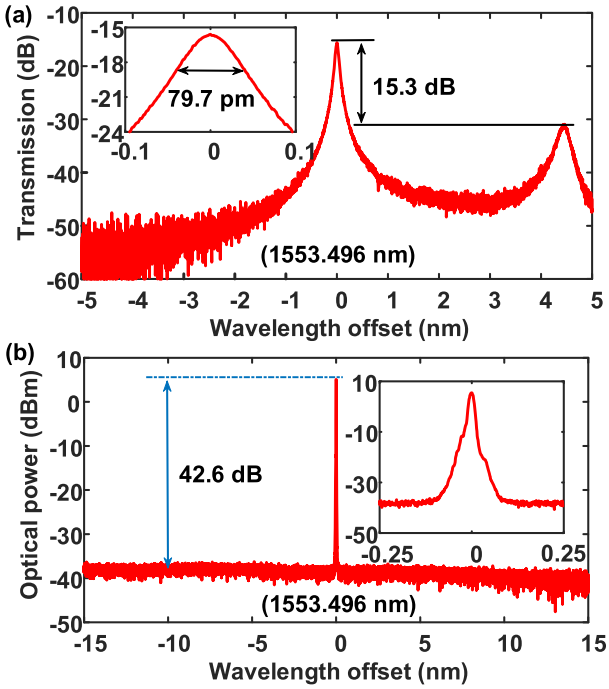

Fig. 3. (a) The measured transmission spectrum at the drop port when the light wave is coupled into the input port. (b) The measured optical spectrum of the generated light by the proposed PT-symmetric optical fiber laser.

The OBPF has a center wavelength of 1555 nm and a 3-dB bandwidth of 10 nm, which is actually a commercial waveshaper (Finisar, Wave Shaper 4000S). The MDR is fabricated based on a standard silicon photonics foundry process. It contains a disk with a diameter of 10 μm, two bus waveguides with a width of 600 nm, and a slab waveguide with a height of 90 nm. Both the disk and the bus waveguides have an identical height of 220 nm. The coupling gap between the disk and the bus waveguides is 200 nm. The temperature of the MDR is controlled by using a temperature controller (ILX Lightwave LTD-5910B). The lasing mode and the linewidth of the output are analyzed through a delayed self-heterodyne system with a 10-km fiber delay line. Note that a 1-GHz signal is used to shift the modes of one heterodyne channel by 1 GHz to make the observation of the beating signals more easily seen. The optical spectra of the generated optical signal are measured through an optical spectrum analyzer (Ando AQ6317B). The electrical spectra of the electrical signal in the delayed self-heterodyne system are evaluated by an electrical spectrum analyzer (Agilent E4448A). The transmission spectra at the drop ports of the dual-waveguide MDR are measured by an optical vector network analyzer (LUNA, OVA 5000).

Figure 3(a) shows the measured transmission spectra at the drop ports of the MDR at a temperature of 24 °C. The center wavelength and the 3-dB bandwidth of the passband for the MDR are measured to be 1553.496 nm and 79.7 pm, respectively. By tuning PC1 and PC2 to balance the gain and loss of the two equivalent loops, single-mode lasing is achieved. The optical spectrum at the output of the PT-symmetric laser is measured at a temperature of 24 °C, as shown in Fig. 3(b). The lasing

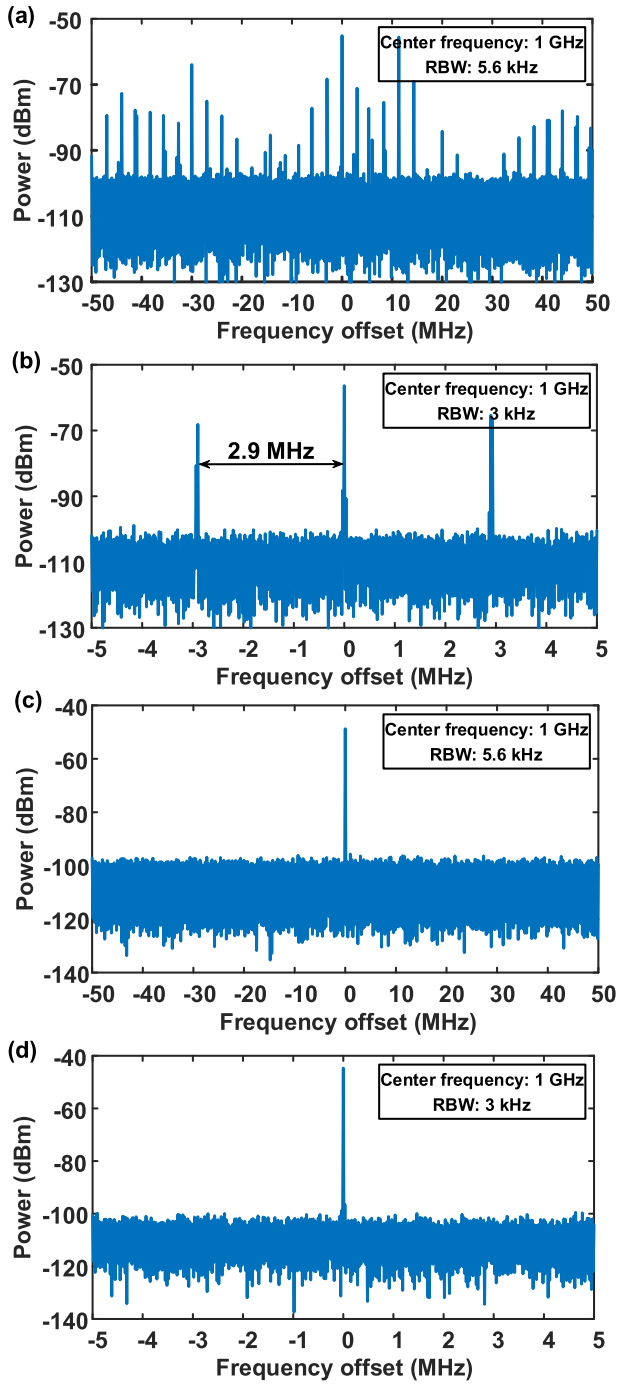

Fig. 4. The measured electrical spectra by the delayed self-heterodyne method when the PT-symmetric optical fiber laser is (a), (b), not under PT-symmetry condition, and (c), (d) under PT-symmetry condition. (a) Span: 100 MHz, RBW: 5.6 kHz. (b) Span: 10 MHz, RBW: 3 kHz. (c) Span: 100 MHz, RBW: 5.6 kHz. (d) Span: 10 MHz, RBW: 3 kHz.

wavelength is 1553.496 nm, which is determined by the center wavelength of the passband of the MDR. The side-mode suppression ratio is measured to be 42.6 dB. A zoom-in view of the optical spectrum is also shown in Fig. 3(b).

To verify that single-mode lasing is implemented due to the mode selection of the PT symmetry, the self-heterodyne radio-frequency (RF) spectrum at the output of the laser is measured,

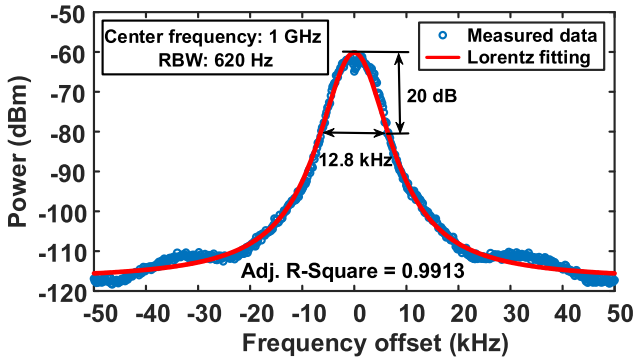

Fig. 5. Self-heterodyne RF spectrum at the output of the optical fiber laser under PT-symmetry condition.

as shown in Fig. 4. At 1553.496 nm, the RF spectra without PT symmetry are shown in Figs. 4(a) and (b) with two different spans of 100 and 10 MHz, respectively. A series of closely spaced beat signals with an FSR of 2.9 MHz are found, which means multi-mode lasing occurs in the laser. By adjusting the polarization states of the light waves entering the Sagnac loop, the gain and loss of the two loops are matched, and the PT symmetry condition is satisfied. The spectra of the RF signals are shown in Figs. 4(c) and (d). There is not a beat signal found except the signal with the shift frequency of 1 GHz, neither in a span of 100 MHz in Fig. 4(c) nor in a span of 10 MHz in Fig. 4(d). A stable single-mode lasing is achieved.

The linewidth is then evaluated by using the delayed self-heterodyne method. The spectrum of the RF signal is measured through an electrical spectrum analyzer (ESA), and the ESA is in the average-mode of 100 times. The measurements are shown in Fig. 5. Excellent agreement is found between the measured data and the Lorentz fitted curve with an adjusted *R*-Square of 0.9913. Considering the unavoidable 1/*f* noise at the center frequency caused by the long loop line [27], the linewidth of the laser is evaluated from the 20-dB spectrum width of the Lorentz fitting curve. The measured 20-dB Lorentz linewidth is 12.8 kHz, corresponding to a 3-dB linewidth of 640 Hz. Theoretically, the exact linewidth of a laser with a sub-kHz level should be measured by using an over 1000-km optical delay line to achieve completely incoherent mixing of the signals from the two arms in a Mach-Zehnder interferometer, because the interference effect will lead to the broadening of the self-heterodyne spectrum. However, it is impossible to obtain a pure Lorentz linewidth spectrum due to the limitation of the laser power and 1/*f* frequency noise [28]. Thus, considering the fitted result is affected by the unavoidable broadening effects, we believe the measured linewidth of 640 Hz is larger than the actual linewidth.

The wavelength tunability of the PT-symmetric fiber laser is also evaluated. By thermally tuning the temperature of the MDR from 17 to 32 °C with a step of 1 °C, the optical spectra at the output of the PT-symmetric laser are recorded, which are shown in Fig. 6(a). Figure 6(b) shows the center wavelength and the output power as a function of temperature. A linear relationship between the wavelength and the temperate is seen.

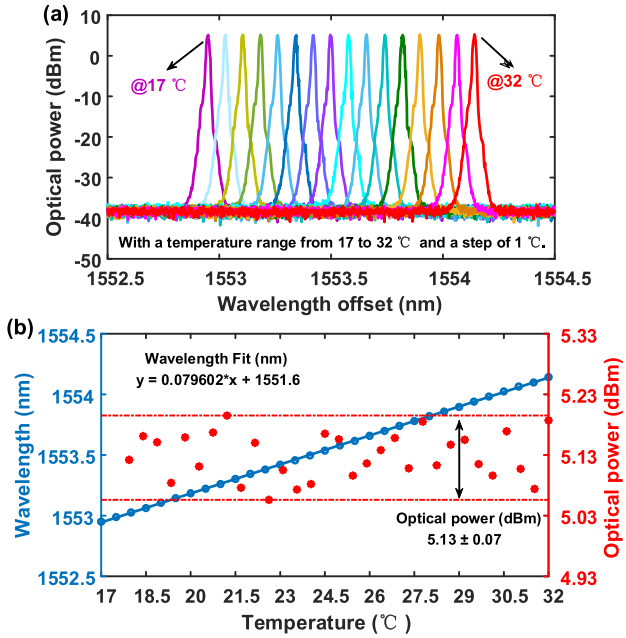

Fig. 6. The tunability of the proposed PT-symmetric optical fiber laser. (a) The measured optical spectra when the temperature of the MDR is tuned from 17 to 32 °C with a step of 1 °C. (b) The wavelength and the optical power as a function of temperature.

The wavelength tuning range is from 1552.953 to 1554.147 nm, and the tuning slope is 79.602 pm/°C. During the wavelength tuning, the output power is measured to be 5.13 dBm with a slight fluctuation of ±0.07 dB.

IV. Conclusion

In summary, a wavelength-tunable single-mode optical fiber laser with a sub-kHz linewidth with PT symmetry implemented by manipulating the polarization states in a single optical loop was proposed and experimentally demonstrated. Thanks to the PT symmetry, an extremely high enhancement in the gain contrast between the broken PT-symmetric mode and all the other unbroken PT-symmetric modes was achieved, which made the fiber laser to operate in stable single mode. The key to achieve PT symmetry in the fiber laser was to manipulate the polarization states of two light waves traveling in the Sagnac loop, to make the gain and loss of the two loops identical in magnitude. The wavelength tuning of the proposed laser was achievedby thermally tuning the MDR. In the experiment, stable single-mode lasing with a wavelength tuning range from 1552.953 to 1554.147 nm and a sub-kHz linewidth of 640 Hz was demonstrated. The demonstration opens new avenues to implement PT-symmetric systems with reduced complexity for potential applications in photonic systems [29], [30] and microwave photonic systems [13], [15].

Appendix

A. Parity-Time Symmetry Equations

In practice, the PT symmetry may be exactly satisfied for one pair of modes, but the other modes deviate from exactly

PT-symmetry conditions. However, as shown in the following analysis, the ability of the mode suppression is still retained for the proposed PT-symmetric optical fiber laser when partial modes of the proposed system deviate from exactly PT-symmetric conditions. By assuming the primary mode is in the exact PT condition and the next competing mode is in the critical condition (the gain/loss balance is skewed), we have

$$\omega_0^{(1,2)} = \omega_0 \pm \sqrt{\kappa_0^2 - g_0^2} \tag{6}$$

$$\omega_1^{(1,2)} = \omega_1 + i\frac{g_{a_1} + g_{b_1}}{2} \pm \sqrt{\kappa_1^2 - \left(\frac{g_{a_1} - g_{b_1}}{2}\right)^2} \tag{7}$$

If the next competing mode undergoes conjugate amplifying/decaying, we have

$$\sqrt{\kappa_1^2 - \left(\frac{g_{a_1} - g_{b_1}}{2}\right)^2} = 0 \tag{8}$$

Since the small mode spacing between the primary mode and the next competing mode, we may assume that the coupling coefficients for the two modes are equal. Then, if the primary mode is in the PT-symmetric broken condition, and the next competing mode is under the critical condition, the gain contrast between the two modes can be rewritten as [14]

$$\hat{\gamma}_{PT} = \sqrt{g_0^2 - \left(\frac{g_{a_1} - g_{b_1}}{2}\right)^2} \tag{9}$$

Then, in consideration of the gain contrast in a single-loop optical fiber laser, which is given by

$$\hat{\gamma}_s = g_0 - g_{a_1} \tag{10}$$

The enhancement factor for the gain contrast can be rewritten as

$$\hat{G} = \frac{\hat{\gamma}_{PT}}{\hat{\gamma}_s} = \frac{\sqrt{g_0^2 - \left(\frac{g_{a_1} - g_{b_1}}{2}\right)^2}}{g_0 - g_{a_1}} \tag{11}$$

Clearly, the enhancement factor $\hat{G}$ grows monotonically if $g_0 > g_{a1}$ and $g_{a1} > -g_{b1}$. Similar to the enhancement factor G for perfect PT-symmetric conditions, the enhancement factor $\hat{G}$ is diverging in the limit of $g_{a1} \to g_0$.

B. Delayed Self-Heterodyne Method

Figure 7 shows the schematic diagram of the delayed self-heterodyne method based on a Mach-Zehnder interferometer structure. The light wave from the proposed optical fiber laser is transmitted through an isolator (ISO2) and divided into two branches by an optical divider (OD). In the upper branch, the light wave is coupled into a phase modulator (PM) via a polarization controller (PC3). In the PM, the light wave is modulated by a microwave signal with a frequency of 1 GHz generated by a microwave source (MS). This can shift the detection frequency away from zero to make the observation of the beating signals more easily seen. In the lower branch, the light wave is launched into a long fiber with a length of around 10 km via a second polarization controller (PC4). The output light waves of the PM

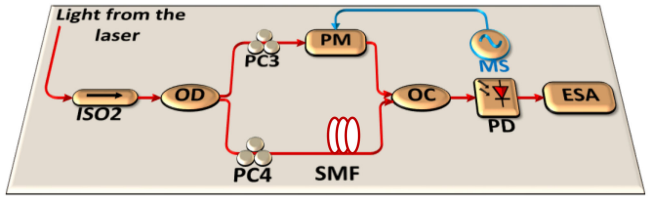

Fig. 7. Schematic diagram of the delayed self-heterodyne method. ISO: isolator; OD: optical divider; PC: polarization controller; PM: phase modulator; SMF: single-mode fiber; OC: optical coupler; PD: photodetector; ESA: electrical spectrum analyzer.

and the long fiber are then combined together via an optical coupler (OC) and detected by a photodetector (PD). The output signal of the PD is analyzed through an electrical spectrum analyzer (ESA).

In the delayed self-heterodyne method, its measurement resolution is given by [31],

$$\Delta f_{res} = \frac{c}{nL_d} \tag{12}$$

where Δf_{res} is the measurement resolution, c is the velocity of light in a vacuum with a value of 299792485 m/s, n is the effective refractive index of the fiber with a value of 1.4566, and L_d is the length of the optical fiber delay line.

If the length of the fiber delay line is 10 km, the measurement resolution would be 20.6 kHz. Theoretically, the exact linewidth of the laser with sub-kHz levels should be measured using an over 1000-km optical fiber delay line to achieve completely incoherent mixing of the ligh waves from the two arms in the Mach-Zehnder interferometer, because the interference effect will lead to the broadening of the self-heterodyne spectrum. In fact, it is impossible to obtain a pure Lorentz linewidth spectrum due to the limitation of the laser power and 1/*f* frequency noise [27], [28]. Thus, considering the fitted result mixing the unavoidable broadening effects mentioned above and the well Lorentz fitted spectrums, the measured linewidth for the proposed PT-symmetric laser will be larger than the real value. Consequently, the measured linewidth can be regarded as the conservative character of the laser linewidth for the proposed PT-symmetric laser.

To verify the ability of the delayed self-heterodyne system with a 10-km fiber delay line for linewidth measurement, the linewidths of two commercial laser sources (Yokogawa AQ2201 and Anritsu MG9638A) are measured, as shown in Fig. 8. In the experiment, the PM (JDSU, Model: 10023874) has a 3-dB bandwidth of 20 GHz. The PD (New Focus, Model:1414) has a 3-dB bandwidth of 25 GHz. The electrical spectra of the electrical signal are evaluated by an electrical spectrum analyzer (Agilent E4448A). Considering the unavoidable 1/*f* noise at the center frequency caused by the long delay line, the linewidth of the lasers is evaluated from the 20-dB spectrum width of the fitting curves. The 20-dB Gauss linewidth of Yokogawa AQ2201 and Lorentz linewidth of Anritsu MG9638A are measured to be 3.717 and 3.32 MHz, corresponding to 3-dB linewidths of 185.85 and 166 kHz, respectively. The measured results are

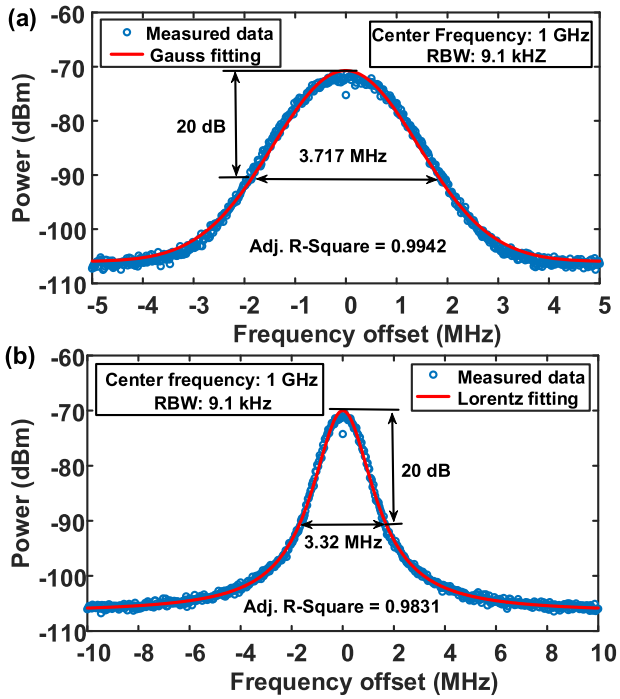

Fig. 8. The measured linewidth of two commercial laser sources. (a) Yokogawa AQ2201 and (b) Anritsu MG9638A.

matched well with the real values, indicating that the system has good linewidth measurement ability.

REFERENCES

[1] C. M. Bender and S. Boettcher, "Real spectra in non-Hermitian Hamiltonians having PT symmetry," *Phys. Rev. Lett.*, vol. 80, no. 24, pp. 5243–5246, Jun. 1998.

[2] C. M. Bender, "Making sense of non-Hermitian Hamiltonians," *Rep. Prog. Phys.*, vol. 70, no. 6, pp. 947–1018, May 2007.

[3] L. Feng, R. El-Ganainy, and L. Ge, "Non-Hermitian photonics based on parity-time symmetry," *Nat. Photon.*, vol. 11, no. 12, pp. 752–762, Nov. 2017.

[4] R. El-Ganainy, K. G. Makris, M. Khajavikhan, Z. H. Musslimani, S. Rotter, and D. N. Christodoulides, "Non-Hermitian physics and PT symmetry," *Nat. Phys.*, vol. 14, no. 1, pp. 11–19, Jan. 2018.

[5] B. Qi, H. Z. Chen, L. Ge, P. Berini, and R. M. Ma, "Parity–time symmetry synthetic lasers: physics and devices," *Adv. Opt. Mater.*, vol. 7, Sep. 2019, Art. no. 1900694.

[6] H. Hodaei, M. A. Miri, M. Heinrich, D. N. Christodoulides, and M. Khajavikhan, "Parity-time-symmetric microring lasers," *Science*, vol. 346, no. 6212, pp. 975–978, Nov. 2014.

[7] L. Feng, Z. J. Wong, R. M. Ma, Y. Wang, and X. Zhang, "Single-mode laser by parity-time symmetry breaking," *Science*, vol. 346, no. 6212, pp. 972–975, Nov. 2014.

[8] H. Hodaei *et al.*, "Parity-time-symmetric coupled microring lasers operating around an exceptional point," *Opt. Lett.*, vol. 40, no. 21, pp. 4955–4958, Nov. 2015.

[9] H. Hodaei *et al.*, "Single mode lasing in transversely multi-moded PT-symmetric microring resonators," *Laser Photon. Rev.*, vol. 10, no. 3, pp. 494–499, Apr. 2016.

[10] M. Brandstetter *et al.*, "Reversing the pump dependence of a laser at an exceptional point," *Nat. Commun.*, vol. 5, Jun. 2014, Art. no. 4034.

[11] W. Liu *et al.*, "An integrated parity-time symmetric wavelength-tunable single-mode microring laser," *Nat. Commun.*, vol. 8, May 2017, Art. no. 15389.

[12] Z. Fan, W. Zhang, Q. Qiu, and J. Yao, "Observation of PT-symmetry in a fiber ring laser," *Opt. Lett.*, vol. 45, no. 4, pp. 1027–1030, Feb. 2020.

[13] Y. Liu, T. Hao, W. Li, J. Capmany, N. Zhu, and M. Li, "Observation of parity-time symmetry in microwave photonics," *Light: Sci. Appl.*, vol. 7, pp. 1–9, Jul. 2018.

[14] J. Zhang and J. Yao, "Parity-time–symmetric optoelectronic oscillator," *Sci. Adv.*, vol. 4, Jun. 2018, Art. no. eaar6782.

[15] Z. Fan, W. Zhang, Q. Qiu, and J. Yao, "Widely tunable parity-time-symmetric optoelectronic oscillator based on a silicon microdisk resonator," in *Proc. Int. Topical Meeting Microw. Photon*, 2019, pp. 1–4.

[16] Y. D. Koninck, G. Roelkens, and R. Baets, "Electrically pumped 1550 nm single mode III-V-on-silicon laser with resonant grating cavity mirrors," *Laser Photon. Rev.*, vol. 9, no. 2, pp. L6–L10, Mar. 2015.

[17] Z. S. Liu, B. Y. Liu, S. H. Wu, Z. G. Li, and Z. J. Wang, "High spatial and temporal resolution mobile incoherent Doppler lidar for sea surface wind measurements," *Opt. Lett.*, vol. 33, no. 13, pp. 1485–1487, Jul. 2008.

[18] D. T. Spencer *et al.*, "An optical-frequency synthesizer using integrated photonics," *Nature*, vol. 557, no. 7703, pp. 81–85, Apr. 2018.

[19] M. G. Suh, Q. F. Yang, K. Y. Yang, X. Yi, and K. J. Vahala, "Microresonator soliton dual-comb spectroscopy," *Science*, vol. 354, no. 6312, pp. 600–603, Nov. 2016.

[20] M. T. Hill *et al.*, "Lasing in metallic-coated nanocavities," *Nat. Photon.*, vol. 1, no. 10, pp. 589–594, Sep. 2007.

[21] M. Khajavikhan *et al.*, "Thresholdless nanoscale coaxial lasers," *Nature*, vol. 482, no. 7384, pp. 204–207, Feb. 2012.

[22] J. T. Kringlebotn, J. L. Archambault, L. Reekie, and D. N. Payne, "Er 3+: Yb 3+-codoped fiber distributed-feedback laser," *Opt. Lett.*, vol. 19, no. 24, pp. 2101–2103, Dec. 1994.

[23] M. Nakamura, K. Aiki, J. Umeda, and A. Yariv, "CW operation of distributed-feedback GaAs-GaAlAs diode lasers at temperatures up to 300 K," *Appl. Phys. Lett.*, vol. 27, no. 7, pp. 403–405, Oct. 1975.

[24] S. F. Liew, B. Redding, L. Ge, G. S. Solomon, and H. Cao, "Active control of emission directionality of semiconductor microdisk lasers," *Appl. Phys. Lett.*, vol. 104, Jun. 2014, Art. no. 231108.

[25] A. L. Schawlow and C. H. Townes, "Infrared and optical masers," *Phys. Rev.*, vol. 112, pp. 1940–1949, Dec. 1958.

[26] Z. Fan, Z. Dai, W. Zhang, Q. Qiu, and J. Yao, "A single-loop PT-symmetric sub-kHz fiber laser based on an integrated microdisk resonator," in *Proc. Opt. Fiber Commun. Conf.*, Mar. 2020, Art. no. W2A.11.

[27] L. B. Mercer, "1/f frequency noise effects on self-heterodyne linewidth measurements," *J. Lightw. Technol.*, vol. 9, no. 4, pp. 485–493, Apr. 1991.

[28] T. Feng, M. Wang, X. Wang, F. Yan, Y. Suo, and X. S. Yao, "Switchable 0.612-nm-spaced dual-wavelength fiber laser with sub-kHz linewidth, ultra-high OSNR, ultra-Low RIN, and orthogonal polarization outputs," *J. Lightw. Technol.*, vol. 37, no. 13, pp. 3173–3182, Jul. 2019.

[29] Y. H. Lai, Y. K. Lu, M. G. Suh, Z. Yuan, and K. Vahala, "Observation of the exceptional-point-enhanced Sagnac effect," *Nature*, vol. 576, no. 3, pp. 65–69, Dec. 2019.

[30] M. P. Hokmabadi, A. Schumer, D. N. Christodoulides, and M. Khajavikhan, "Non-Hermitian ring laser gyroscopes with enhanced Sagnac sensitivity," *Nature*, vol. 576, pp. 70–74, Dec. 2019.

[31] P. Horak and W. H. Loh, "On the delayed self-heterodyne interferometric technique for determining the linewidth of fiber lasers," *Opt. Express*, vol. 14, no. 9, pp. 3923–3928, May 2006.

Zhiqiang Fan received the B.Eng. degree in electronic science and technology (optoelectronic engineering and optical communication) from the University of Electronic Science and Technology of China (UESTC), Chengdu, China, in 2015. He is currently working toward the Ph.D. degree with the School of Optoelectronic Science and Engineering, UESTC. He is a joint Ph.D. student with the Microwave Photonics Research Laboratory, School of Electrical Engineering and Computer Science, University of Ottawa, Ottawa, ON, Canada.

His current research interests include photonic generation of microwave waveforms and integrated microwave photonics.

Zheng Dai received the B.Eng. degree in electrical engineering and automation from Northwestern Polytechnical University, Xi'an, China, in 2015. He is currently working toward the MA.Sc. degree with the Microwave Photonics Research Laboratory, School of Electrical Engineering and Computer Science, University of Ottawa, Ottawa, ON, Canada.

His current research interests including parity-time symmetry and its applications in microwave photonics.

Qi Qiu received the B.S. degree in laser technology from the Huazhong University of Science and Technology, Wuhan, China and the Ph.D. degree in optical engineering from the University of Electronic Science and Technology of China (UESTC), Chengdu, China, in 1985 and 2007, respectively. He is currently a Professor with UESTC. He has authored more than 100 international journals and conferences.

His current research interests include optical communication, microwave photonics, and optical fiber sensor.

Jianping Yao (Fellow, IEEE) received the Ph.D. degree in electrical engineering from the Université de Toulon et du Var, Toulon, France, in 1997. He is a Distinguished University Professor and the University Research Chair with the School of Electrical Engineering and Computer Science, University of Ottawa, Ottawa, ON, Canada. From 1998 to 2001, he was with the School of Electrical and Electronic Engineering, Nanyang Technological University, Singapore, as an Assistant Professor. In 2001, he joined the School of Electrical Engineering and Computer Science, University of Ottawa as an Assistant Professor, where he was promoted to Associate Professor in 2003, and a Full Professor in 2006. He was appointed the University Research Chair in Microwave Photonics in 2007. In 2016, he was conferred the title of Distinguished University Professor at the University of Ottawa. From 2007 to 2010 and from 2013 to 2016, he was the Director of the Ottawa-Carleton Institute for Electrical and Computer Engineering.

He has authored or coauthored more than 620 research papers including-more than 360 papers in peer-reviewed journals and more than 260 papers in conference proceedings. He is an Editor-in-Chief for the *IEEE Photonics Technology Letters*, a Topical Editor of *Optics Letters*, an Associate Editor for *Science Bulletin*, a Steering Committee Member of the IEEE JOURNAL OF LIGHTWAVE TECHNOLOGY, and an Advisory Editorial Board Member of *Optics Communications*. He was a Guest Editor of a Focus Issue on Microwave Photonics in Optics Express in 2013, a Lead-Editor of a Feature Issue on Microwave Photonics in Photonics Research in 2014, and a Guest Editor of a Special Issue on Microwave Photonics in the IEEE JOURNAL OF LIGHTWAVE TECHNOLOGY in 2018. He is currently the Chair of the IEEE Photonics Ottawa Chapter and is the Technical Committee Chair of IEEE MTT-3 Microwave Photonics. He was a member of the European Research Council Consolidator Grant Panel in 2016, the Qualitative Evaluation Panel in 2017, and a member of the National Science Foundation Career Awards Panel in 2016. He was also the Chair of a number of international conferences, symposia, and workshops, including the Vice Technical Program Committee (TPC) Chair of the 2007 IEEE Topical Meeting on Microwave Photonics, TPC Co-Chair of the 2009 and 2010 Asia-Pacific Microwave Photonics Conference, TPC Chair of the High-Speed and Broadband Wireless Technologies Subcommittee of the IEEE Radio Wireless Symposium 2009–2012, TPC Chair of the Microwave Photonics Subcommittee of the IEEE Photonics Society Annual Meeting 2009, TPC Chair of the 2010 IEEE Topical Meeting on Microwave Photonics, General Co-Chair of the 2011 IEEE Topical Meeting on Microwave Photonics, TPC Co-Chair of the 2014 IEEE Topical Meetings on Microwave Photonics, and General Co-Chair of the 2015 and 2017 IEEE Topical Meeting on Microwave Photonics. He was also a committee member for a number of international conferences, such as IPC, OFC, BGPP, and MWP. He is the recipient of the 2005 International Creative Research Award of the University of Ottawa, the 2007 George S. Glinski Award for Excellence in Research, a Natural Sciences and Engineering Research Council of Canada Discovery Accelerator Supplements Award in 2008, an inaugural OSA Outstanding Reviewer Award in 2012, and the Award for Excellence in Research 2017-2018 at the University of Ottawa. He was one of the top ten reviewers of IEEE/OSA JOURNAL OF LIGHTWAVE TECHNOLOGY (2015–2016). He was an IEEE MTT-S Distinguished Microwave Lecturer for 2013–2015. He is a registered Professional Engineer of Ontario. He is a Fellow of the Optical Society of America, the Canadian Academy of Engineering, and the Royal Society of Canada.